Carbon Nanolights in Piezopolymers are Self-Organizing Toward Color Tunable Luminous Hybrids for Kinetic Energy Harvesting

Xuebing He, Chuanfeng Wang, Xi Huang, Long Jin, Xiang Chu, Meilin Xie, Yiwen Nie, Yali Xu, Zhou Peng, Chaoliang Zhang, Jun Lu,* and Weiqing Yang*

Herein, an all-solid-state sequential self-organization and self-assembly process is reported for the in situ construction of a color tunable luminous inorganic/polymer hybrid with high direct piezoresponse. The primary inorganic self-organization in solid polymer and the subsequent polymer self-assembly are achieved at high pressure with the first utilization of piezo-copolymer (PVDF-TrFE) as the host matrix of guest carbon quantum dots (CQDs). This process induces the spontaneous formation of a highly ordered, microscale, polygonal, and hierarchically structured CQDs/PVDF-TrFE hybrid with multicolor photoluminescence, consisting of very thermodynamic stable polar crystalline nanowire arrays. The electrical polarization-free CQDs/PVDF-TrFE hybrids can efficiently harvest the environmental available kinetic mechanical energy with a new large-scale group-cooperation mechanism. The open-circuit voltage and short-circuit current outputs reach up to 29.6 V cm^{-2} and 550 nA cm^{-2}, respectively. The CQDs/PVDF-TrFE–based hybrid nano-generator demonstrates drastically improved durable and reliable features during the real-time demonstration of powering commercial light emitting diodes. No attenuation/fluctuation of the electrical signals is observed for ≈10 000 continuous working cycles. This study may offer a new design concept for progressively but spontaneously constructing novel multiple self-adaptive complex inorganic/polymer hybrids that promise applications in the next generation of self-powered autonomous optoelectronic devices.

1. Introduction

The definition of a new field of chemistry, "supramolecular chemistry," has been proposed by the Nobel Laureate Jean-Marie Lehn.[1] The area subsequently developed into the chemistry of "self-organization" and more recently toward "adaptive chemistry," dynamic networks, and complex systems.[1] Being considered as a sort of ultimate synthetic chemistry, supramolecular/noncovalent and molecular/covalent self-organization drives the formation and evolution of complex matters in our universe, spanning from molecules to life to thinking organism.[1,2] Passive, thermodynamically controlled, or, active, out-of-equilibrium, dissipative self-organization occurs in response to external or internal stimuli/effectors.[1] This follows a multistep pathway toward the progressive construction of the final nano-, micro-, and macrostructural motifs from their components.[1] Particularly, if the subunits involved possess specific biological, optical, electrical, and magnetic properties, the spontaneous but controlled self-ordering may induce the generation of a range of novel features in the complex systems.[1]

As self-organization processes play a key role in the efficient production of highly ordered functional systems, they have been massively explored concerning the organic, inorganic, and organic–inorganic hybrid entities with molecular- and mesoscale periodicities.[1–16] Among these, the self-organizations of inorganics in polymers are of particular interest, which could lead to the construction of previously unknown functional materials with elaborate hybridized structures.[3–5] Exciting progress has been made in recent years.[3–5] For example, the dynamic reorganization of gold nanoparticles under stress resulted in the formation of a conductive cellular network pathway in polyurethane matrix. This enabled the electronic tunability of the mechanical properties of the stretchable conductors.[3] Also, aragonite nanorods were formed in calcium carbonate/poly(vinyl alcohol) hybrids through self-organization processes from amorphous calcium carbonate solution.[4] Moreover, nacre-like fibers, with high stretchability and gravimetric toughness, were produced by shear-induced solid state self-organization of graphene nanosheets in poly(vinyl alcohol).[5] Nevertheless, with the available constitution, structure and energy combinations, the controllable in situ construction of nano- and mesoscale

X. He, C. Wang, X. Huang, L. Jin, X. Chu, M. Xie, Y. Nie,
Y. Xu, Z. Peng, Prof. J. Lu, Prof. W. Yang
Key Laboratory of Advanced Technologies of Materials
Ministry of Education
School of Materials Science and Engineering
Southwest Jiaotong University
Chengdu 610031, Sichuan, China
E-mail: junluprc@hotmail.com; wqyang@swjtu.edu.cn
C. Zhang
State Key Laboratory of Oral Diseases
West China Hospital of Stomatology
Sichuan University
Chengdu 610041, Sichuan, China

The ORCID identification number(s) for the author(s) of this article can be found under https://doi.org/10.1002/smll.201905703.

ADVANCED
SCIENCE NEWS
www.advancedsciencenews.com

NANO · MICRO
small
www.small-journal.com

self-organized heterotextured electro-optical architectures still remains one of the great challenges in the realization of complex inorganic-polymer hybrid systems with diverse functions.

Carbon quantum dots (CQDs), an emerging star of carbon nanomaterials, are attracting considerable attention in the field of optoelectronics and energy storage/conversion, owing mainly to their unique physiochemical, optical, and electronic properties.[14,17–30] CQDs combine favorable attributes of tunable photoluminescence (PL), resistance to photobleaching and simple synthetic routes without incurring the burden of elemental scarcity.[14,17–30] Their advantages have introduced them as a nontoxic and environmentally friendly alternative to traditional heavy-metal–based quantum dots (QDs).[14,17–30] CQDs are quasispherical nanoparticles, with ultrafine sizes below 10 nm, and they can be amorphous or nanocrystalline with sp^2 carbon clusters.[14,17–30] PL emission is the predominant property of CQDs, and they present excitation wavelength-independent[19,22,25] and excitation wavelength-dependent[18,19,22,24,25] fluorescence with different PL colors. Being asserted as the next big small things, these emergent carbon nanolights hold great promise to serve as inorganic building blocks for future optoelectronic nanohybrids and nanodevices, though the research is still at the early stage.[14,17–30]

Kinetic mechanical energy is prevalent everywhere we live, which exists in various forms, such as human movement, object vibration, water flow, wind whispering, and so forth. Consequently, effective conversion of mechanical energy into electricity is of critical importance for the sustainable operation of self-powered electronic devices and systems.[29–37] Diversified approaches have been developed via the mechanisms of electromagnetic induction, electrostatic generation, or piezoelectric effect.[29–37] Especially, piezoelectric nanogenerators (PNGs) show more advantages in capturing the dynamic mechanical energy with variable amplitudes and frequencies.[29–37] Recent advances in PNGs focus on boosting power generation/conversion efficiency and developing hybridized piezoelectric materials for multiple adaptive electronics and optoelectronics.[29,30,33,34,36,37]

Piezoelectric polymers, poly(vinylidene fluoride) (PVDF), and its copolymer, poly(vinylidene fluoride-co-trifluoroethylene) (PVDF-TrFE), have demonstrated significant potential in PNGs because of their good structural flexibility and excellent mechanical sensitivity.[34–48] Similar to PVDF, PVDF-TrFE is a semicrystalline polymer with at least four polymorphs (α, β, γ, and δ).[35–48] The content and structure of crystalline β phase is responsible for its piezoresponse magnitude.[35–48] However, homopolymer PVDF generally crystallizes in nonpolar α phase, whereas copolymer PVDF-TrFE readily crystallizes into polar β phase regardless of processing method.[35–48] The introduction of TrFE co-monomer into VDF sterically hinders the formation of a trans-gauche-trans-gauche (tg^+tg^-) configuration.[35–48] It forces the molecular chains into an all-trans ($tttt$) conformation (β phase).[35–48] Therefore, the presence of TrFE makes PVDF-TrFE copolymer a stronger candidate than its homopolymer predecessor in constructing self-powered optoelectronic micro/nanohybrids of high power generation and multiple adaptiveness.
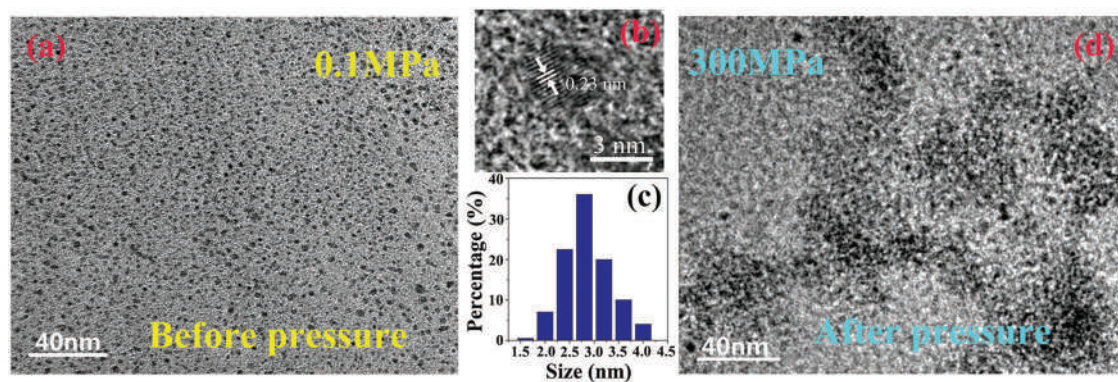
In this work, we develop an all-solid-state sequential self-organization and self-assembly strategy for the in situ construction of a color tunable luminous complex inorganic/polymer hybrid system with high direct piezoresponse. This is realized at high pressure with the first utilization of piezoelectric copolymers as the host matrix of luminescent carbon nanodots guest. Pressure drives the self-organization of CQDs in solid PVDF-TrFE, and the self-organized CQDs further induce the self-assembly of PVDF-TrFE chains. This process leads to the spontaneous formation of numerous highly thermodynamic stable microscale CQDs/PVDF-TrFE hybrid nanowire array patterns with crystalline β phase. The CQDs hybridized PVDF-TrFE exhibited fluorescent colors varying from blue, green, and yellow to red, depending on the light excitation wavelengths. Being assembled as an electrical polarization-free PNG, the micro/nanoscale hierarchically structured polar crystalline CQDs/PVDF-TrFE hybrids could efficiently harvest the environmental available kinetic mechanical energy into electricity with a new large-scale group-cooperation working mechanism. The maximum open-circuit voltage and short-circuit current output density, generated from direct piezoelectric responses, reached up to 29.6 V cm^{-2} and 550 nA cm^{-2}, respectively. During the real time demonstration of the powering of commercial light emitting diodes (LEDs), the CQDs/PVDF-TrFE–based PNGs displayed very good durability and stability. No attenuation of the electrical output signals was observed for ≈10 000 cycles continuous working.

2. Results and Discussion

Prior to high pressure treatment, transmission electron microscopy (TEM) was utilized to reveal the dispersion and morphology of CQDs in the CQDs/PVDF-TrFE blends, fabricated by the solution casting approach at normal pressure. For the blend samples with CQDs content of 1–3 wt%, the TEM images show that uniform and monodispersed CQDs are embedded in PVDF-TrFE (**Figure 1**a; and Figure S1, Supporting Information). The CQDs are crystalline, as proven by the oriented lattice fringes in the enlarged views of high resolution TEM (HRTEM) (Figure 1b). The lattice spacings are calculated to be ≈0.23 nm, similar to that of diamond.[17–28] Figure 1c shows the CQDs in a CQDs/PVDF-TrFE (3/97, wt/wt) blend are dispersed in narrow size distribution with an average diameter of 2.84 nm. Nevertheless, the serious agglomeration of CQDs occurs when the CQDs content is increased above 4 wt%. This is shown in the typical TEM of a CQDs/PVDF-TrFE (4/96, wt/wt) blend, prepared with the same solution casting process (Figure S2a, Supporting Information). The HRTEM of the agglomerated CQDs is shown in Figure S2b, Supporting Information. It evidently reveals the well-resolved, intrinsic, characteristic crystalline lattice structure of the CQDs.

Figure 1a,d shows a comparison of the typical TEM micrographs of the as fabricated CQDs/PVDF-TrFE (3/97, wt/wt) hybrid samples, before and after the applied high-pressure treatment. As can be seen, the CQDs, with the size in a few nanometers, were uniformly dispersed in the polymer matrix, just through the delicate solution casting process (Figure 1a). More interestingly, the fluorescent CQDs at high pressure managed to assemble together in PVDF-TrFE. Unique self-organized micro/nanoscale architectures of CQDs were clearly

**ADVANCED
SCIENCE NEWS**

www.advancedsciencenews.com

**NANO · MICRO
small**

www.small-journal.com

Figure 1. a) TEM of the CQDs/PVDF-TrFE (3/97, wt/wt) blend, prepared by the solution casting approach at normal pressure. b) HRTEM of a typical CQD, embedded in the PVDF-TrFE matrix, with a lattice spacing of 0.23 nm. c) Size distribution of CQDs in the PVDF-TrFE, obtained by counting about 200 HRTEM imaged particles, before the applied high pressure processing. d) TEM of the CQDs/PVDF-TrFE (3/97, wt/wt) hybrid sample, after the high pressure treatment at 300 MPa, 240 °C for 60 min.
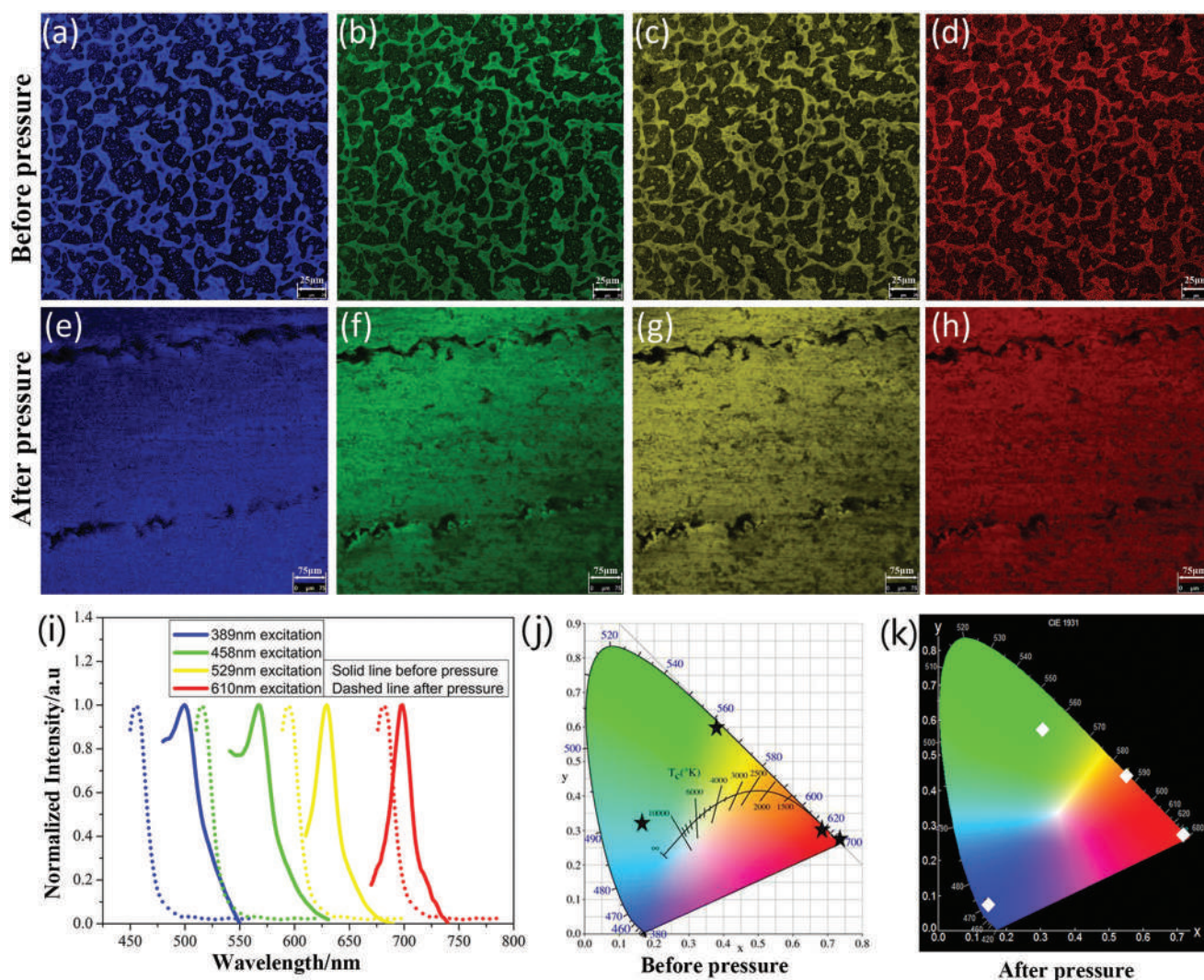
observed when the same hybrid sample was processed at 300 MPa, 240 °C for 60 min (Figure 1d).

The original CQDs show excitation wavelength-dependent PL emissions. When the excitation wavelength is increased from 360 to 660 nm with a uniform difference of 20 nm, the PL emission peak shifts from 500 to 714 nm (Figure S3, Supporting Information). The absolute photoluminescent quantum yields (PL QYs) of the CQDs are determined to be 48.95% for blue emission, 48.44% for green emission, 24.23% for yellow emission, and 8.27% for red emission, under the excitations at 389, 458, 529, and 610 nm, respectively (Table S1, Supporting Information). **Figure 2**a–h gives out the laser scanning confocal microscope (LSCM) images of the CQDs/PVDF-TrFE (3/97, wt/wt) hybrid samples before and after the processing at high pressure, excited at the different excitation wavelengths. Prior to the pressure treatment, the CQDs/PVDF-TrFE film exhibited color tunable PL properties transferred from CQDs, emitting blue, green, yellow, and red fluorescent lights, under the excitations of violet, green, yellow, and red visible lights, respectively (Figure 2a–d). Astonishingly, the color tunable PL properties were well maintained in the CQDs/PVDF-TrFE hybrid sample even if it has endured the self-organization process of CQDs at high pressure. As shown in Figure 2e–h, the self-organized CQDs/PVDF-TrFE hybrid still demonstrated the same multicolor photoluminescence effect, with the variation of the light excitation wavelengths. Before pressure treatment, the PL QYs of CQDs/PVDF-TrFE are determined to be 38.68% for blue emission, 32.92% for green emission, 15.43% for yellow emission, and 8.57% for red emission, under the excitations at 389, 458, 529, and 610 nm, respectively (Table S1, Supporting Information). After pressure treatment, the PL QYs of CQDs/PVDF-TrFE are determined to be 27.39% for blue emission, 32.84% for green emission, 10.19% for yellow emission, and 6.35% for red emission, under the excitations at 389, 458, 529, and 610 nm, respectively (Table S1, Supporting Information). This demonstrates these excitation wavelength-dependent pressure-treated CQDs/PVDF-TrFE still possess respectable multicolor emission efficiencies in a rather broad wavelength region.[24] It is adequate for some appealing applications that require color tunable fluorescence emissions, such as multidimensional sensing

and multicolor bioimaging.[23–25] Based on the representative PL spectra of the CQDs/PVDF-TrFE, the emission peaks centered at 510, 572, 625, and 710 nm, before pressure treatment, and centered at 455, 513, 592, and 680 nm, after pressure treatment, when the hybrids were irradiated by the excitations at the exactly the same wavelengths of 389, 458, 529, and 610 nm, respectively (Figure 2i). The chromaticity coordinates in the CIE (Commission Internationale de L'Eclairage) maps (Figure 2j,k), computed from the CQDs/PVDF-TrFE at the 389, 458, 529, and 610 nm excitations, were consistent with the observations from the PL and LSCM tests. Recent results have shown the luminescence origination from CDs to be surface related intrinsic luminescence.[27] Therefore, the irreversible blueshift PL may also indicate the occurrence of the interaction between PVDF-TrFE molecules and CQDs surfaces in the pressure treated CQDs/PVDF-TrFE.[27]

Figure 3 displays a set of differential scanning calorimetry (DSC), wide angle X-ray diffraction (WAXD), and attenuated total reflectance Fourier transform infrared spectroscopy (ATR-FTIR) characterization results for the CQDs/PVDF-TrFE hybrids, with various contents of CQDs, crystallized at 300 MPa, 240 °C for 60 min. As can be seen from the DSC diagram (Figure 3a), the melting point of PVDF-TrFE decreased slightly with the addition of 1 wt% CQDs. Nevertheless, with the further increase of CQDs content, the melting point gradually increased. When the CQDs content reached 3 wt%, the melting temperature of the CQDs/PVDF-TrFE hybrid was 153.56 °C, which is around 21 °C higher than that of pure PVDF-TrFE. According to the simplified Thomson–Gibbs equation,[49] the higher melting point suggested crystalline ordering structures of PVDF-TrFE, with more thermodynamic stability, were formed in the hybrid system, resulting from the self-organization of CQDs at high pressure. The crystal forms of the polymer in the hybrids were subsequently determined by WAXD and ATR-FTIR. With reference to X-ray diffraction data (Figure 3b), the distinct Bragg reflection peak at the 2θ angle of 19°–20°, corresponding to the (110)/(200) lattice planes, indicated the presence of crystalline β phase PVDF-TrFE for all the hybrid samples.[45–48] As for IR spectra (Figure 3c), the prominent characteristic bands associated with polar β-phase, at the wavelengths of 840, 1286, and 1430 cm^{-1}, respectively, further

ADVANCED
SCIENCE NEWS
www.advancedsciencenews.com

NANO · MICRO
small
www.small-journal.com

Figure 2. LSCM images of the CQDs/PVDF-TrFE (3/97, wt/wt) hybrids a–d) before and e–h) after high pressure processing, obtained at a,e) violet, b,f) blue, c,g) green, and d,h) red excitations, respectively, and typical i) PL spectra and j,k) CIE diagram of CQDs/PVDF-TrFE, under 389, 458, 529, and 610 nm excitations, respectively.
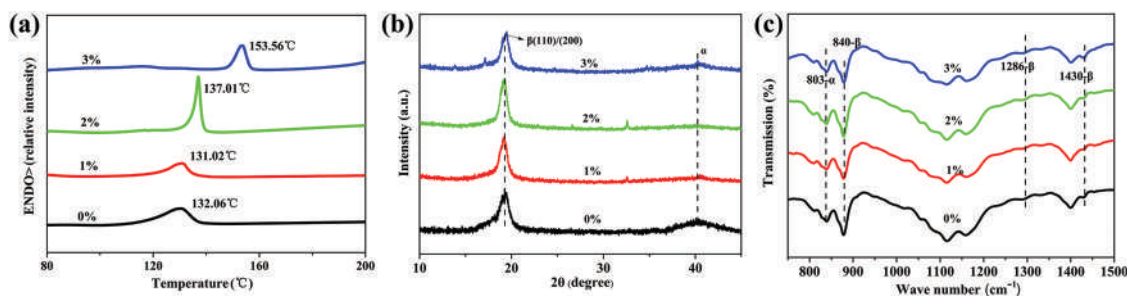
confirmed the *β* phase of the polymer in the pressure crystallized hybrids.[45–48]

Figure 4 shows the typical scanning electron microscopy (SEM) images of the etched fracture cross sections of the pressure processed CQDs/PVDF-TrFE hybrids. Different crystalline structures, within micro- and nanoscale, were observed with the variation of component ratios. For the CQDs/PVDF-TrFE (1/99, wt/wt) sample, disorderly petal-like nanosheets were revealed, together with their microscale assemblies (Figure 4a–c). When 2 wt% CQDs were introduced into PVDF-TrFE, the petal nanosheets began to appear in an orderly state. Also, the 3D micro-/nanorod assemblies replaced those nanosheet assemblies once existed (Figure 4d–f). No petal-like nanosheets were found in the CQDs/PVDF-TrFE (3/97, wt/wt) sample. Amazingly, many hexagonal structures, with tens of micrometers in size, were developed instead. A close observation demonstrated that they were actually assembled from highly ordered nanowire arrays (Figure 4g–i). Consistent with the DSC, WAXD,

and ATR-FTIR results, the SEM further suggested that the crystalline ordering in the hybrids increased with the increase of CQDs content. Particularly, with the appropriate constitution and energy combinations, very thermodynamic stable hierarchically structured polar crystalline CQDs/PVDF-TrFE hybrids, highly ordered within both micro- and nanoscale, could be formed through the evolution of CQDs self-organization.

For reference, the pristine PVDF-TrFE sample was also crystallized exactly at 300 MPa, 240 °C for 60 min. With the same etching process, SEM only revealed the ordinary crystalline lamellae of PVDF-TrFE on the fracture surface, which were formed through the normal bulk crystallization of the polymer. No trace of such micro/nanoscale nanosheets or nanowires was observed in the sample (Figure S4, Supporting Information). This indicates the CQDs play an important role in the formation of the highly ordered and polar crystalline micro/nanoarchitectures. The previous study on the CQDs/PVDF blends has shown the CQDs were well dispersed before

**ADVANCED
SCIENCE NEWS**

www.advancedsciencenews.com
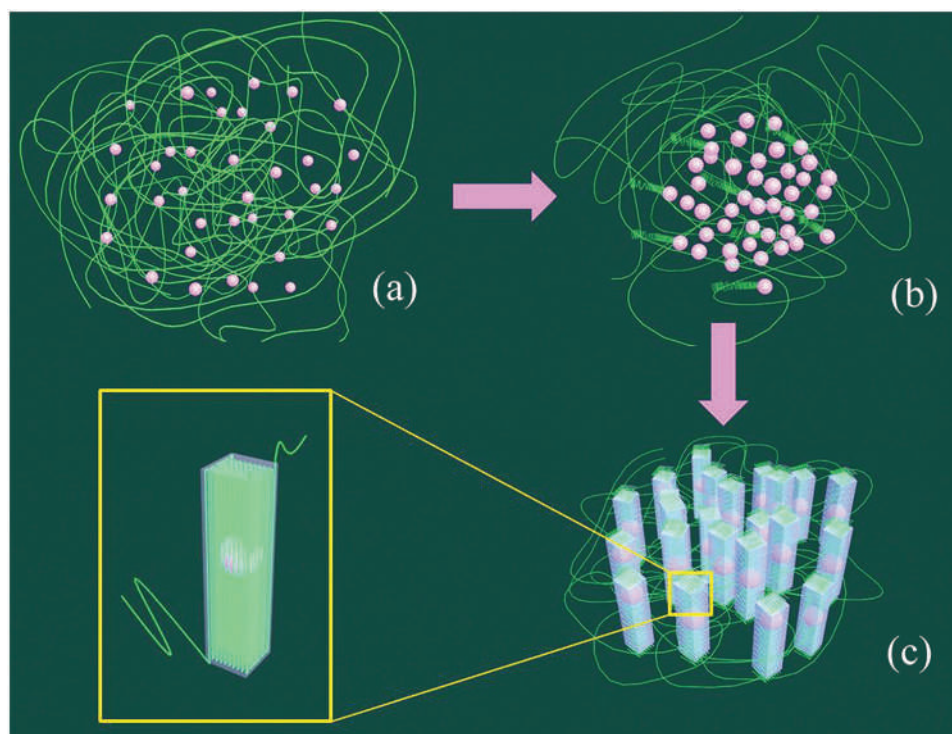
NANO · MICRO

small

www.small-journal.com

Figure 3. a) DSC, b) WAXD, and c) ATR-FTIR graphs of the CQDs/PVDF-TrFE hybrids, with different contents of CQDs, crystallized at 300 MPa, 240 °C for 60 min.

and after the high pressure crystallization.[29] As a result, the formed PVDF nanosheets or nanowires were evenly distributed in the samples without the further formation of their micro/nanoscale hierarchical assemblies.[29] Therefore, the growth of the nanowire arrays assembled micro/nanoscale hexagonal hybrid structures in CQDs/PVDF-TrFE (Figure 4g–i) should be closely related with the dynamic formation process of the self-organized micro/nanoarchitectures of CQDs at high pressure (Figure 1d).

Considering the TEM and SEM observations, the formation of the color tunable luminous micro/nanoscale hierarchical hybrids in Figure 4g–i, might be assigned to the sequential CQDs self-organization and the subsequent PVDF-TrFE self-assembly processes at high pressure.[29,37–40,50,51] This is schematically described in **Figure 5**. Initially, the CQDs are uniformly distributed in PVDF-TrFE matrix (Figure 5a). Working in collaboration with the molecular chains of the piezo-copolymer PVDF-TrFE, the applied pressure drives the
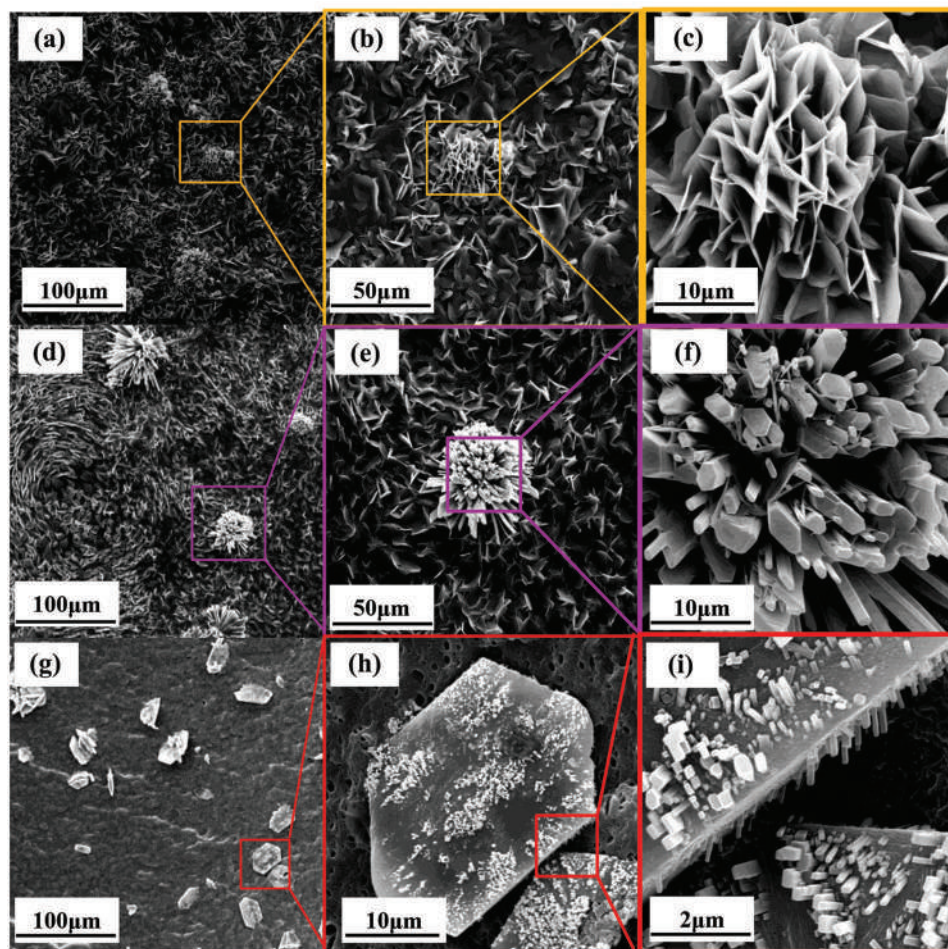
Figure 4. SEM micrographs of the CQDs/PVDF-TrFE hybrids, with different component ratios, crystallized at 300 MPa, 240 °C for 60 min. CQDs/PVDF-TrFE: a–c) 1/99, wt/wt; d–f) 2/98, wt/wt; g–i) 3/97, wt/wt. (b,e,h) and (c,f,i) are partial enlargements of (a,d,g) and (b,e,h), respectively.

ADVANCED
SCIENCE NEWS
www.advancedsciencenews.com

NANO · MICRO
small
www.small-journal.com

Figure 5. a–c) Schematic illustration of the in situ formation process of the microscale CQDs/PVDF-TrFE nanowire array pattern at high pressure. Working in coordination with PVDF-TrFE, pressure drives the self-organization of CQDs, and the self-organized CQDs further induce the self-assembly of PVDF-TrFE. This process leads to the spontaneous growth of a thermodynamic stable hybrid nanowire array pattern with multicolor luminescence.

self-organization of the glowing CQDs. Then the self-organized CQDs patterns evolve inside PVDF-TrFE within microscale (Figure 5b). The self-organized CQDs further induce the molecular self-assembly of the copolymer chains at high pressure. They play as a catalyst, similar to the role of the molten gallium walls in the growth of highly aligned silica nanowires[50] or the stannum particles in the formation of zinc oxide nanowires.[51] As the sensitivity of different phase transitions to pressure is different, the increased pressure may shift the phase equilibrium of the system, and then bring a new axis to the self-assembly space.[38–40] This finally leads to the growth of the highly ordered and thermodynamically stable polar crystalline hybrid nanowire arrays of CQDs/PVDF-TrFE. Notably, they are assembled in a microscale polygonal form and with multicolor luminescence (Figure 5c).

What needs to be noticed here is that the initial dispersion state of CQDs in piezopolymer matrices is very critical to the final polar crystalline structures formed at high pressure. If the CQDs have seriously agglomerated before pressure treatment, they will directly induce the self-assembly of piezopolymer molecules at high pressure, without the dynamic self-organization of the CQDs agglomerations, thus forming a 3D architecture with a low structural ordering, followed by a relatively low piezoresponse.[29,39] This is disadvantageous for further boosting the power generation/conversion efficiency of PNGs by direct piezoelectric response.[29,39] Therefore, the initial monodispersion of CQDs in solid piezopolymers is one of the essential prerequisites for the above sequential self-organization and self-assembly process, which may further lead to the

formation of highly ordered organic/polymer hybrids with high direct piezoresponse.

Being assembled as PNGs, the kinetic energy harvesting properties of the self-organized CQDs/PVDF-TrFE hybrids were evaluated without any treatment of electrical poling. **Figure 6** shows the electrical output comparison of the hybrid PNGs, with the variation of CQDs and PVDF-TrFE component ratio. The electrical outputs were generated at a stimulating frequency of 1.0 Hz and applied force of 20 N. For the single PVDF-TrFE, its open-circuit voltage and short-circuit current density outputs were 2.6 V cm^{-2} and 30 nA cm^{-2}, respectively. But as we expected, the open-circuit voltage and short-circuit current outputs, created from direct piezoelectric responses, gradually increased with the increase of CQDs content. In particular, the voltage and current output density for the CQDs/PVDF-TrFE (3/97, wt/wt) hybrid, reached 11.5 V cm^{-2} and 235 nA cm^{-2}, around 4.5 times and 8 times the values of single PVDF-TrFE, respectively. The results indicated that the higher the polar crystalline ordering of the hybrid structures, the higher the efficiency of electromechanical conversion. Therefore, the controllable in situ construction of micro/nanoscale heterotextured CQDs/PVDF-TrFE hybrids, shining with desirable mechanical-to-electrical conversion, was realized with a pressure-driven self-organization process of monodispersed CQDs.

Further studies showed the direct piezoelectric responses of the self-organized CQDs/PVDF-TrFE hybrids could be tuned by the frequency variation of stimulated dynamic force. **Figure 7**a,b displays the electrical outputs of the CQDs/PVDF-TrFE

ADVANCED
SCIENCE NEWS
www.advancedsciencenews.com

NANO · MICRO
small
www.small-journal.com
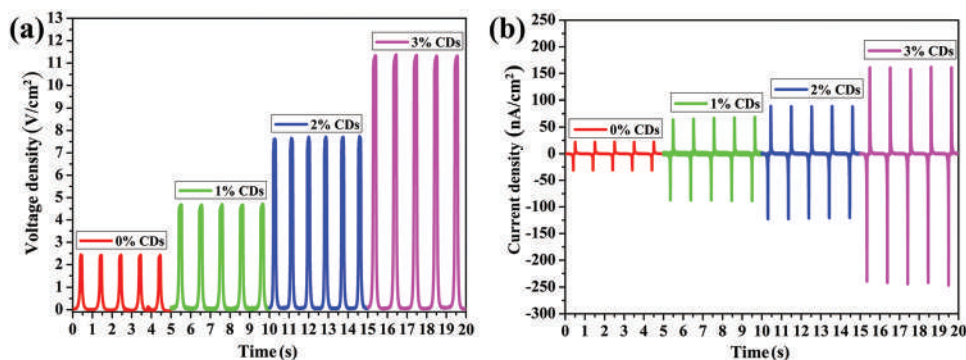
Figure 6. a) Open-circuit voltage and b) short-circuit current outputs of the CQDs/PVDF-TrFE hybrids with various component ratio, generated at a stimulating frequency of 1.0 Hz and applied force of 20 N.

(1/99, wt/wt)–based PNG. It was stimulated at a given force of 20 N, with the frequency varied from 1.0, 1.5, 2.0, and 2.5 to 3.0 Hz. Both the voltage and current outputs increased step by step with the increase of loading frequency. The open-circuit voltage and short-circuit current output density, increased from 4.8 V cm^{-2} and 68 nA cm^{-2} at 1.0 Hz to 15 V cm^{-2} and 550 nA cm^{-2} at 3.0 Hz, respectively. This suggested that the piezo-responses of the CQDs/PVDF-TrFE hybrids were very self-adaptive to the alteration of dynamic frequency. Consequently, this enabled them to scavenge energy from the diversified and irregular kinetic motions in a practical environment. Moreover, with their ability of frequency self-adaptiveness, the electrical outputs of the hybridized PNGs might be further optimized with the appropriate increase of stimulated frequency, especially for the one in which highly ordered hybrid structures

were developed through the CQDs self-organization processes. Figure 7c,d shows the electrical outputs of the CQDs/PVDF-TrFE (3/97, wt/wt) hybrid subject to 4.0 Hz loading frequency and 20 N loading force. The generated voltage and current density outputs reached 29.4 V cm^{-2} and 550 nA cm^{-2}, respectively. To our knowledge, the measured piezoelectric voltage output density, originating from the poling free CQDs/PVDF-TrFE hybrid, surpassed that of state-of-the-art piezopolymers reported to date.

So far, starting from solid state inorganic/polymer systems, the self-organized and/or self-assembled electro-optical inorganic-polymer heterotextures have been prepared by the self-organization of nanostructured inorganics in organic polymers, without the following organic polymer self-assembly.[3–5] Otherwise, they were fabricated by inducing organic polymer
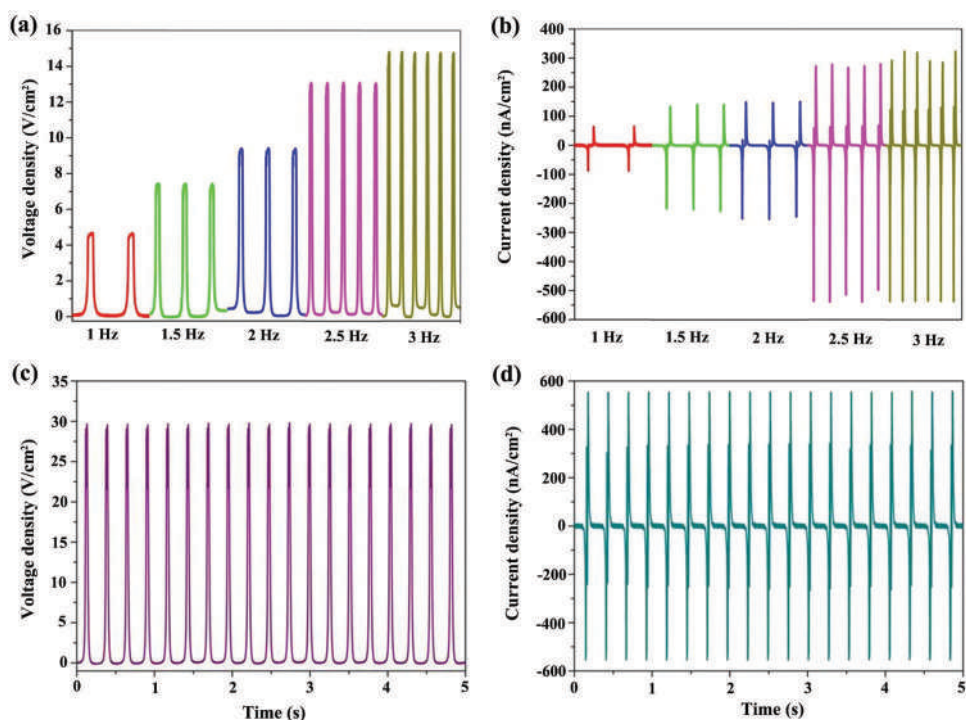
Figure 7. Open-circuit voltage (left) and short-circuit current (right) outputs of the CQDs/PVDF-TrFE hybrids, stimulated at different frequencies and a given force of 20 N: a,b) CQDs/PVDF-TrFE (1/99, wt/wt), from 1.0 to 3.0 Hz; c,d) CQDs/PVDF-TrFE (3/97, wt/wt), 4.0 Hz.

**ADVANCED
SCIENCE NEWS**
www.advancedsciencenews.com

**NANO · MICRO
small**
www.small-journal.com

self-assembly with uniformly dispersed inorganic nanostructures, without the preceding inorganic self-organization.[29] The self-organization of inorganics or the self-assembly of organic polymers is separate, isolated, and not related together.[3–5,29] In the previous report on CQDs/PVDF, the CQDs were well dispersed in the homopolymer PVDF, before and after the applied high pressure treatment.[29] There was a lack of the dynamic CQDs self-organization during the pressure crystallization.[29] The evenly distributed CQDs simply induced the self-assembly of the homopolymer chains.[29] This led to the growth of nanosheet or nanowire structures without the further formation of their micro/nanoscale assemblies.[29] For the CQDs/PVDF hybrids, the maximum open-circuit voltage output density reached 19.2 V cm^{-2}.[29] In the current study on CQDs/PVDF-TrFE, the adding of TrFE copolymer triggered at high pressure the dynamic self-organization of the initially monodispersed CQDs. Then the unique self-organized micro/nanoscale architectures of CQDs were formed (Figure 1). The self-organized CQDs in turn induced the self-assembly of the TrFE copolymer chains. This led to the spontaneous formation of a highly ordered, microscale, polygonal, and hierarchically structured CQDs/PVDF-TrFE hybrid, consisting of very thermodynamic stable polar crystalline nanowire arrays (Figure 4g–i). It is an unreported dynamic but sequential inorganic self-organization and the subsequent organic self-assembly process that proceeds progressively in the solid state inorganic/organic system. For the CQDs/PVDF-TrFE hybrids, the voltage output density was improved to 29.4 V cm^{-2} (Figure 7c,d). It is 1.5 times that of their CQDs/PVDF counterparts. Also, it is the highest direct piezoelectric response reported in the open literature. More importantly, the current study on CQDs/PVDF-TrFE may offer a new design concept for the progressive but spontaneous construction of novel multiple self-adaptive complex inorganic/polymer hybrids that promise applications in self-powered autonomous optoelectronic devices.

The enhancement of the direct piezoresponse could be explained by the voltage/power generation mechanism of the hybridized piezoelectric structures.[29,52,53] In the previous publication, a CQDs/PVDF–based hybrid PNG was developed.[29] Although the polar crystalline nanosheet structures were formed, there was a lack of their micro/nanoscale assemblies in the PNG.[29] Its power generation was ascribed to the deformation and the subsequent relaxation of the piezoelectric nanosheets that just evenly distributed inside.[29] In the current research, as discussed above, the sequential CQDs self-organization and PVDF-TrFE self-assembly at high pressure lead to the spontaneous construction of the numerous microscale "colorful polygon nanogenerators" in the polymer matrix. They are assembled from the highly thermodynamic stable polar crystalline nanowire arrays. It is known the cooperation of the unique material structure design with intrinsic material properties play a key role to achieve the desired functionalities.[54] Particularly, the micro-/nanoscale dual structures have proved their significance in improving the properties and functions of biological organisms, such as self-cleaning lotus leaves, antifogging mosquito eyes, and so on.[54] Hence, the improved power generation of the CQDs/PVDF-TrFE hybrid PNG should be attributed to the large-scale group cooperation of the huge amounts of spontaneously constructed but micro/nanoscale hierarchically structured "polygon nanogenerators."

Figure 8a gives out the schematic representation of the power generation process of the CQDs/PVDF-TrFE (3/97, wt/wt)–based hybrid PNG. Initially, there is no polarization on the outside surfaces of the original sample (Figure 8a, stage I). When the vertical compressive force from the mechanical vibrator is applied to the top of the PNG, the nanowire arrays in the "polygonal nanogenerators" begin to deform synergistically. And then, piezoelectric charges are generated. The charges accumulate on both sides of the electrodes, and flow from the lower to the upper electrode under the action of potential difference. This results in an instantaneous positive current signal output (Figure 8a, stage II). Next, the nanowire arrays reach the maximum bending state, and the voltage output exhibits accordingly the maximum potential value (Figure 8a, stage III). The nanowire arrays will return to their original state when the external force is released. The charges flow back, from the upper to the lower electrode. This produces an output signal of negative current (Figure 8a, stage IV). The cycle goes round and round. In this way, a steady and persistent output of electrical signals can be achieved for the hybrid PNG, with the consistent cooperation of a huge number of "polygonal nanogenerators."

The long-term stability issue is one of the major roadblocks for the practical applications of high performance PNGs. Several hybrid materials, consisting of luminescent CQDs as guest and piezoelectric homopolymer as host, were fabricated, and their applications in PNGs were investigated.[29,30,37] However, there was a decrease or increase of electrical output in the long-term operation of these PNGs.[29,30,37] By choosing the short-circuit current output as the main evaluating parameter, the long-term energy harvesting properties of the CQDs/PVDF-TrFE hybrid PNGs were assessed in terms of their performance durability and stability. Figure 8b displays the output current-time curves of the CQDs/PVDF-TrFE (3/97, wt/wt)–based PNG for ≈10 000 continuous hitting cycles, at a stimulated force of 20 N and frequency of 3.0 Hz. Evidently, the hybrid PNG showed exceptionally durable and reliable features in capturing the kinetic mechanical energy, due to the existence of the self-organized structures with high thermodynamic stability. Notably, no decrease/increase of the electrical signals had been observed until the end of the test. The self-organized hybrids were also demonstrated as a power source to operate commercial LEDs. Figure 8c,d gives out the digital pictures of a commercial green LED, being connected to the same PNG, before and after an impact of 3.0 Hz and 20 N, respectively. As can be seen, the LED bulb was lit up successfully. The generated electricity from the hybrid PNG, 8.04 mm in diameter and 0.5 mm in thickness, instantly turned on a total of 11 commercial green LEDs. They kept shining during the durability and stability test described above (Figure 8e).

Our group has reported the fabrication of several hybrid materials with the utilization of piezoelectric homopolymers as the host matrices of carbon nanodots, and the investigation of their application in PNGs.[29,30,37] The current research developed a new hybrid material with the first utilization of piezoelectric copolymers as the host matrix of carbon nanodots. Meanwhile, an all-solid-state sequential self-organization and self-assembly strategy was also first developed for the in situ construction of color tunable luminous inorganic/polymer hybrid systems with high direct piezoresponses. The previously
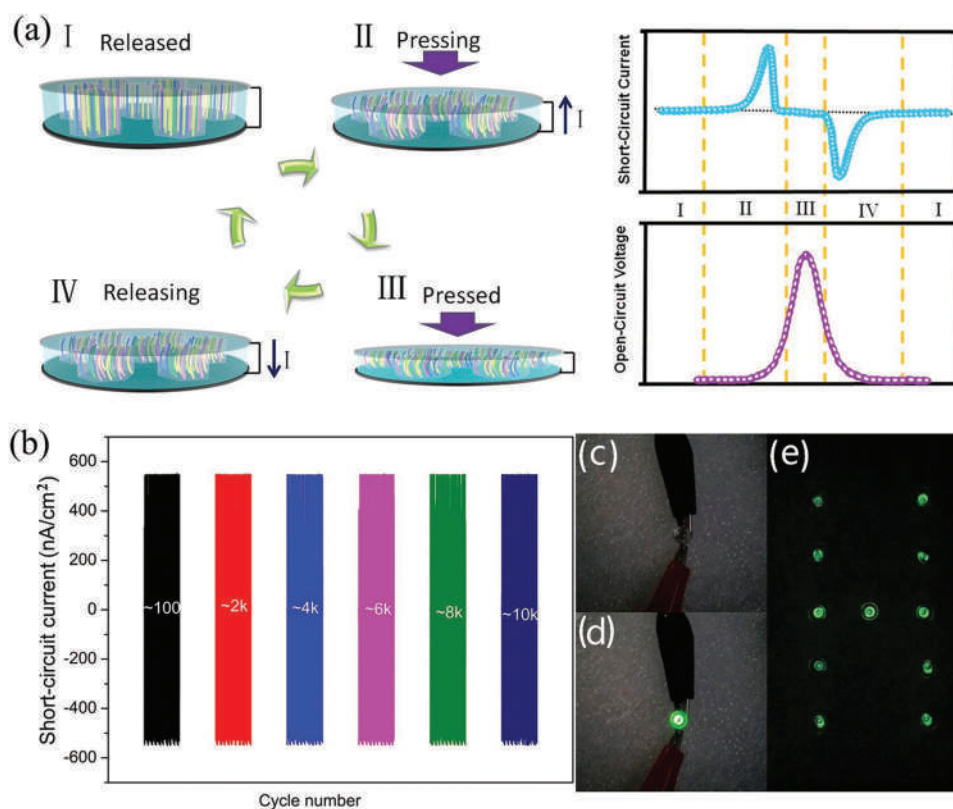
Figure 8. a) Schematic drawing of the composite structure and working mechanism for a CQDs/PVDF-TrFE (3/97, wt/wt)–based hybrid PNG. b) Output current-time curves of the hybrid PNG for ≈10 000 cycles continuous working, whole signal, stimulated by a 3.0 Hz 20 N impact. c–e) Real time demonstration of the powering of commercial LEDs during the stability and durability test. (c) and (d) are digital pictures of a LED, before and after the applied mechanical force, respectively, and (e) shows 11 LEDs operated instantly with the PNG generated power. PNG size: 8.04 mm in diameter and 0.5 mm in thickness.

unreported dynamic but sequential self-organization and self-assembly process led to the spontaneous formation of a highly ordered luminescent piezoelectric hybrid material with increased degrees of complexity. This enabled the PNGs to harvest the kinetic mechanical energy with a new large-scale group-cooperation working mechanism. Compared with the previous CQDs/homopolymer PNGs, the current CQDs/copolymer PNGs exhibited a significant enhancement of direct piezoelectric response. The measured voltage output density value surpassed the highest value of state-of-the-art piezopolymers reported to date. More strikingly, the current CQDs/copolymer PNGs demonstrated drastically improved performance stability in the long-term operation, which is one of bottleneck challenges for practical applications of inorganic/polymer-based PNGs. This may further extend their applications in the field of multidimodal autonomous optoelectronics.

In particular, considering its simplicity and effectiveness, the newly developed strategy may inspire researchers to cross multiple disciplines for further investigations. There is still much room for the improvement in the optoelectric properties of the hybrid materials consisting of luminescent carbon nanodots as guest and piezoelectric copolymers as host. Recently, more and more new CQDs with intriguing luminescence properties and high PL QYs were synthesized with versatile synthesis methods and diverse precursors.[18–28] A combination of the advantages of

these CQDs and the host piezoelectric copolymers may lead to the further boosting of the luminescent properties, power generation/conversion efficiency, and applications of CQDs/polymer hybrids.

3. Conclusions

In summary, we have demonstrated the in situ spontaneous construction of micro-/nanoscale, multiple optoelectronic adaptive, and heterotextured inorganic/polymer architectures via an all-solid-state sequential self-organization and self-assembly process. In particular, a highly ordered, microscale, polygonal, and hierarchically structured CQDs/PVDF-TrFE hybrid, consisting of very thermodynamic stable polar crystalline nanowire arrays, was self-organized with the optimization of constitution and energy combinations. The self-organized CQDs/PVDF-TrFE hybrid exhibited fascinating color tunable photoluminescence, varying from blue, green, and yellow to red, dependent on the light excitation wavelengths. Without any electrical poling process, the CQDs/PVDF-TrFE hybrid–based PNG was capable of efficiently harvesting electrical energy from the ubiquitously distributed kinetic motions with a new large-scale group-cooperation working mechanism. The maximum open-circuit voltage and short-circuit current density outputs, generated by direct piezoelectric responses, reached
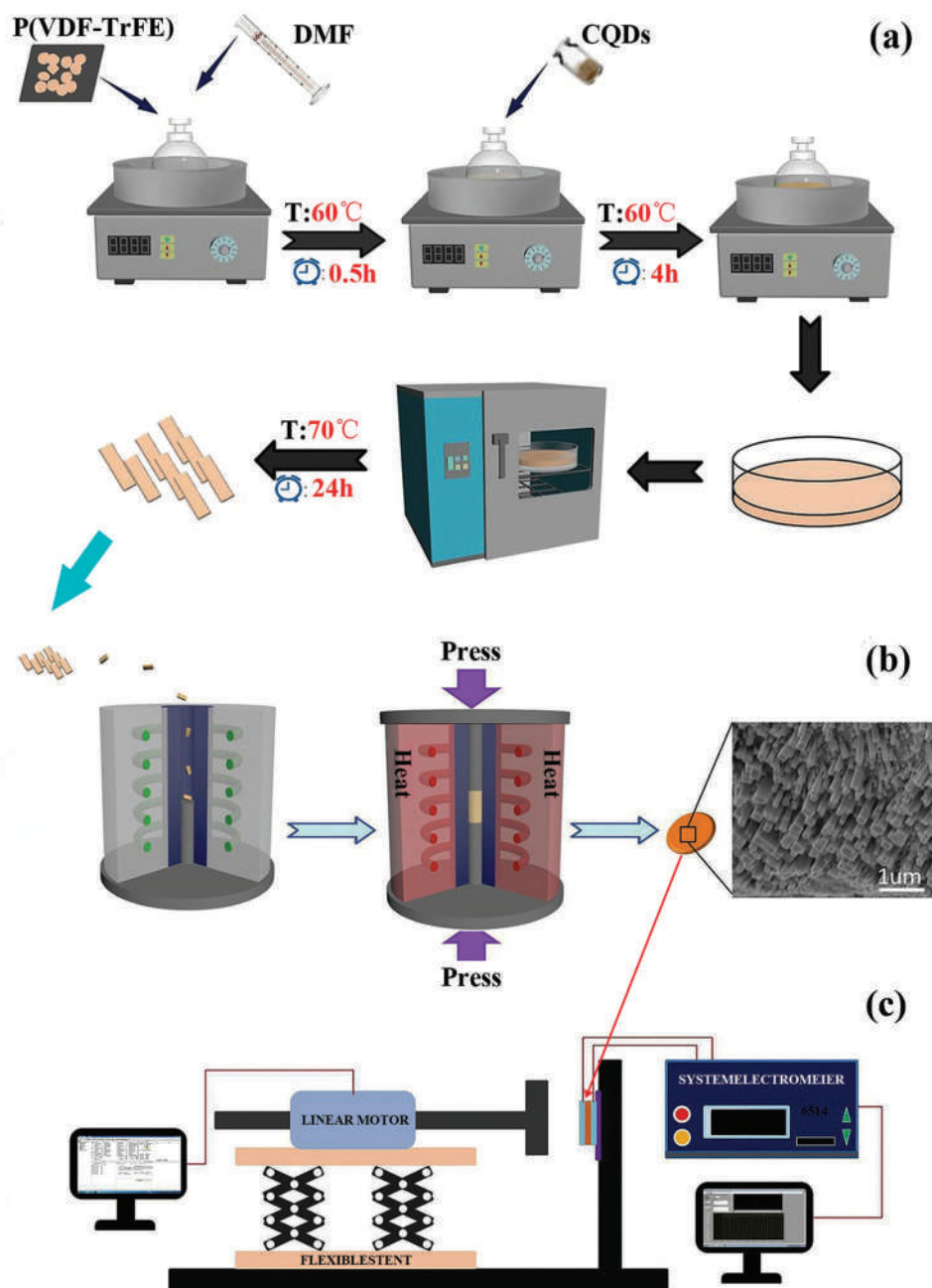
Figure 9. a) Schematic diagram illustrating the mixing process of CQDs and PVDF-TrFE, b) the experimental procedure in fabricating the CQDs/PVDF-TrFE hybrids with a piston-cylinder high-pressure apparatus, and c) the impact measurement system for concurrently collecting the generated electrical potential and current outputs.

up to 29.6 V cm^{-2} and 550 nA cm^{-2}, respectively. Moreover, the hybrid PNG showed exceptionally durable and reliable features as a power source to operate commercial LEDs. No attenuation of the output electrical signals was observed for ≈10 000 continuous working cycles. We believe the as self-organized electro-optical inorganic/polymer hybrid may diversify niche applications in a new-generation of self-powered autonomous photoelectric micro-/nanodevices, with its combined action of high piezoresponse and multicolor luminescence. The present study may possibly open a new avenue for the design and fabrication of novel hybridized piezoelectric materials for multiple self-adaptive electronics and optoelectronics.

4. Experimental Section

CQDs were supplied by Jinnaisi New Materials Co., Ltd, Nanjing, China. PVDF-TrFE (molar ratio, 80/20), with the weight-average molecular

**ADVANCED
SCIENCE NEWS**

www.advancedsciencenews.com

**NANO · MICRO
small**

www.small-journal.com

weight of 100 000 g mol^{-1}, was obtained from Huasen High-Tech Co., Ltd, Shaanxi, China. Analytical grade N, N-dimethylformamide (DMF), concentrated sulfuric acid (H_2SO_4), phosphorus pentoxide (P_2O_5) and chromium trioxide (CrO_3), were provided by Kelong Chemical Co., Ltd, Chengdu, China, and were used as received.

The flow diagram for the mixing process of CQDs and PVDF-TrFE is illustrated in **Figure 9**a. First, PVDF-TrFE was dissolved in DMF, and stirred at 60 °C for 30 min. After the complete dissolution of PVDF-TrFE, CQDs were added to the solution. The mixture was further stirred at the same temperature for additional 4 h to obtain a uniformly mixed solution. Afterward, the mixed solution was coated on a glass substrate and then dried in a vacuum oven at 70 °C for 24 h to remove the DMF solvent. Finally, the dried blend film was shredded and granulated for high pressure treatment.

The as prepared CQDs/PVDF-TrFE blends were subjected to high-pressure processing using a self-developed piston-cylinder apparatus (Figure 9b). The CQDs/PVDF-TrFE granules were filled in the mold when its temperature was raised to 160 °C. Then they were kept under this phase for 10 min to get completely melt. Subsequently, a low pressure (150 MPa) was loaded, and the mold temperature was raised to 240 °C. After the balance was established, the pressure was further increased to 300 MPa. The samples were kept under these conditions for a period of 60 min, and then quenched down to ambient condition at a rate of 2 °C min^{-1}. Three CQDs/PVDF-TrFE hybrid specimens were prepared by varying the CQDs and PVDF-TrFE compositions. They were with a uniform column aspect, 8.04 mm in diameter and 0.50 mm in thickness. For reference, a single PVDF-TrFE sample was also prepared under the same treatment.

TEM observations were performed using a JEOL JEM-2100F device. LSCM observations were conducted with a KEYENCE VK-9700 apparatus. PL spectra was obtained at room temperature utilizing a FLS980 spectrometer (Edinburgh instrument) with a 450 W xenon lamp. The 1931 CIE system was used to calculate the chromaticity coordinates. The absolute PL QYs were measured by using a calibrated integrating sphere attached to the FLS980 spectrometer. DSC testing was performed using a TA-Q20 instrument at standard atmospheric pressure. WAXD results were obtained at room temperature using a DX-1000 diffractometer. ATR-FTIR test was conducted using a Nicolet 5700 spectrometer. SEM images were acquired using a JSM-6330F machine. The sample surfaces were etched before SEM observations, adopting an improved method from Vaughan.[55]

The kinetic energy harvesting performance of the CQDs/PVDF-TrFE hybrid PNGs was evaluated by a periodic impact apparatus (Figure 9c). The NTIAG HS01-37 × 166 linear motor was used as impact source. The generated electrical signals were collected by the Keithley 6514 system electrometer and the Stanford Research SR570 low noise current preamplifier. Switching polarity tests were carried out with standard piezopolymer to verify that the generated electrical signals came directly from the piezoresponses of PNGs, rather than from the influence of measurement system or environment.

Supporting Information

Supporting Information is available from the Wiley Online Library or from the author.

Acknowledgements

Conflict of Interest

The authors declare no conflict of interest.

Author Contributions

X.H., C.W., X.H., and L.J. contributed equally to this work. J.L. is the Lead Contact. J.L. conceived the idea, initiated the study, and organized the entire research. X.H., C.W., X.H., L.J., X.C., M.X., Y.N., Y.X., Z.P., and C.Z. carried out the sample preparation and characterization. X.He., J.L., and W.Y. analyzed and interpreted the data, and wrote the manuscript with the assistance of all other co-authors.

Keywords

[1] a) J. M. Lehn, *Angew. Chem., Int. Ed.* **2013**, *52*, 2836; b) J. M. Lehn, *Isr. J. Chem.* **2018**, *58*, 136.

[2] a) B. Pokroy, S. H. Kang, L. Mahadevan, J. Aizenberg, *Science* **2009**, *323*, 237; b) J. M. A. Carnall, C. A. Waudby, A. M. Belenguer, M. C. A. Stuart, J. J. P. Peyralans, S. Otto, *Science* **2010**, *327*, 1502; c) H. Reinhardt, H. C. Kim, C. Pietzonka, J. Kruempelmann, B. Harbrecht, B. Roling, N. Hampp, *Adv. Mater.* **2013**, *25*, 3313.

[3] Y. Kim, J. Zhu, B. Yeom, M. D. Prima, X. Su, J. G. Kim, S. J. Yoo, C. Uher, N. A. Kotov, *Nature* **2013**, *500*, 59.

[4] S. Kajiyama, T. Nishimura, T. Sakamoto, T. Kato, *Small* **2014**, *10*, 1634.

[5] J. Zhang, W. C. Feng, H. X. Zhang, Z. L. Wang, H. A. Calcaterra, B. Yeom, P. A. Hu, N. A. Kotov, *Nat. Commun.* **2016**, *7*, 10701.

[6] a) S. Ogawa, K. Ashida, T. Kaneko, I. Takahashi, *Mater. Chem. Front.* **2018**, *2*, 2191; b) T. O. Mason, U. Shimanovich, *Adv. Mater.* **2018**, *30*, 1706462.

[7] a) R. B. Rakhi, W. Chen, D. W. Cha, H. N. Alshareef, *Nano Lett.* **2012**, *12*, 2559; b) X. Zhang, Y. Q. Zhao, C. L. Xu, *Nanoscale* **2014**, *6*, 3638; c) D. Kowalski, J. Mallet, J. Michel, M. Molinari, *J. Mater. Chem. A* **2015**, *3*, 6655.

[8] D. J. Yan, X. D. Zhu, K. X. Wang, X. T. Gao, Y. J. Feng, K. N. Sun, Y. T. Liu, *J. Mater. Chem. A* **2016**, *4*, 4900.

[9] M. T. Li, L. Cong, J. Zhao, T. T. Zheng, R. Tian, J. Q. Sha, Z. M. Su, X. L. Wang, *J. Mater. Chem. A* **2017**, *5*, 3371.

[10] P. McCormack, F. Han, Z. J. Yan, *J. Phys. Chem. Lett.* **2018**, *9*, 545.

[11] a) I. Levchenko, U. Cvelbar, M. Modic, G. Filipič, X. X. Zhong, M. Mozetič, K. Ostrikov, *J. Phys. Chem. Lett.* **2013**, *4*, 681; b) D. Cai, L. L. Wang, L. Li, Y. P. Zhang, J. Z. Li, D. Chen, H. R. Tu, W. Han, *J. Mater. Chem. A* **2019**, *7*, 806.

[12] G. Zhang, C. Verdugo-Escamilla, D. Choquesillo-Lazarte, J. M. García-Ruiz, *Nat. Commun.* **2018**, *9*, 5221.

[13] M. Favaro, S. Agnoli, M. Cattelan, A. Moretto, C. Durante, S. Leonardi, J. Kunze-Liebhäuser, O. Schneider, A. Gennaro, G. Granozzi, *Carbon* **2014**, *77*, 405.

[14] S. L. Hu, Y. L. Ding, Q. Chang, A. Trinchi, K. Lin, J. L. Yang, J. Liu, *Nanoscale* **2015**, *7*, 4372.

[15] a) S. Guerra, J. Iehl, M. Holler, M. Peterca, D. A. Wilson, B. E. Partridge, S. D. Zhang, R. Deschenaux, J. F. Nierengarten, V. Percec, *Chem. Sci.* **2015**, *6*, 3393; b) C. Wang, S. Ling, J. Yang, D. Rao, Z. Guo, *Small* **2018**, *14*, 1702072.

ADVANCED
SCIENCE NEWS

www.advancedsciencenews.com

NANO · MICRO
small
www.small-journal.com

[16] J. Y. Lin, B. Liu, M. N. Yu, X. H. Wang, L. B. Bai, Y. M. Han, C. J. Ou, L. H. Xie, F. Liu, W. S. Zhu, X. W. Zhang, H. F. Ling, P. N. Stavrinou, J. P. Wang, D. D. C. Bradley, W. Huang, *J. Mater. Chem. C* **2018**, *6*, 1535.

[17] a) S. N. Baker, G. A. Baker, *Angew. Chem., Int. Ed.* **2010**, *49*, 6726; b) X. T. Zheng, A. Ananthanarayanan, K. Q. Luo, P. Chen, *Small* **2015**, *11*, 1620; c) F. L. Yuan, S. H. Li, Z. T. Fan, X. Y. Meng, L. Z. Fan, S. H. Yang, *Nano Today* **2016**, *11*, 565; d) R. Wang, K. Q. Lu, Z. R. Tang, Y. J. Xu, *J. Mater. Chem. A* **2017**, *5*, 3717; e) J. J. Du, N. Xu, J. L. Fan, W. Sun, X. J. Peng, *Small* **2019**, *15*, 1805087; f) X. X. Shi, H. M. Meng, Y. Q. Sun, L. B. Qu, Y. H. Lin, Z. H. Li, D. Du, *Small* **2019**, *15*, 1901507; g) X. T. Tian, X. B. Yin, *Small* **2019**, *15*, 1901803; h) X. X. Ye, Y. H. Xiang, Q. R. Wang, Z. Li, Z. H. Liu, *Small* **2019**, *15*, 1901673.

[18] a) D. Qu, M. Zheng, L. G. Zhang, H. F. Zhao, Z. G. Xie, X. B. Jing, R. E. Haddad, H. Y. Fan, Z. C. Sun, *Sci. Rep.* **2015**, *4*, 5294; b) X. Miao, D. Qu, D. X. Yang, B. Nie, Y. K. Zhao, H. Y. Fan, Z. C. Sun, *Adv. Mater.* **2018**, *30*, 1704740.

[19] a) Y. Mu, N. Wang, Z. C. Sun, J. Wang, J. Y. Li, J. H. Yu, *Chem. Sci.* **2016**, *7*, 3564; b) J. C. Liu, N. Wang, Y. Yu, Y. Yan, H. Y. Zhang, J. Y. Li, J. H. Yu, *Sci. Adv.* **2017**, *3*, e1603171; c) J. Y. Li, B. L. Wang, H. Y. Zhang, J. H. Yu, *Small* **2019**, *15*, 1805504.

[20] S. Khan, A. Sharma, S. Ghoshal, S. Jain, M. K. Hazra, C. K. Nandi, *Chem. Sci.* **2018**, *9*, 175.

[21] P. Zhao, X. P. Li, G. Baryshnikov, B. Wu, H. Agren, J. J. Zhang, L. L. Zhu, *Chem. Sci.* **2018**, *9*, 1323.

[22] Y. Zhan, B. Shang, M. Chen, L. M. Wu, *Small* **2019**, *15*, 1901161.

[23] a) S. J. Zhu, J. H. Zhang, L. Wang, Y. B. Song, G. Y. Zhang, H. Y. Wang, B. Yang, *Chem. Commun.* **2012**, *48*, 10889; b) J. L. He, Y. L. He, Y. H. Chen, B. F. Lei, J. L. Zhuang, Y. Xiao, Y. R. Liang, M. T. Zheng, H. R. Zhang, Y. L. Liu, *Small* **2017**, *13*, 1700075; c) P. Yang, Z. Q. Zhu, T. Zhang, W. Zhang, W. M. Chen, Y. Z. Cao, M. Z. Chen, X. Y. Zhou, *Small* **2019**, *15*, 1902823.

[24] a) L. L. Pan, S. Sun, A. D. Zhang, K. Jiang, L. Zhang, C. Q. Dong, Q. Huang, A. G. Wu, H. W. Lin, *Adv. Mater.* **2015**, *27*, 7782; b) Z. X. Gan, H. Xu, Y. L. Hao, *Nanoscale* **2016**, *8*, 7794; c) B. van Dam, H. Nie, B. Ju, E. Marino, J. M. J. Paulusse, P. Schall, M. J. Li, K. Dohnalová, *Small* **2017**, *13*, 1702098.

[25] a) H. Ding, P. Zhang, T. Y. Wang, J. L. Kong, H. M. Xiong, *Nanotechnology* **2014**, *25*, 205604; b) H. Ding, J. S. Wei, H. M. Xiong, *Nanoscale* **2014**, *6*, 13817; c) H. Ding, H. M. Xiong, *RSC Adv.* **2015**, *5*, 66528; d) H. Ding, S. B. Yu, J. S. Wei, H. M. Xiong, *ACS Nano* **2016**, *10*, 484; e) H. Ding, J. S. Wei, P. Zhang, Z. Y. Zhou, Q. Y. Gao, H. M. Xiong, *Small* **2018**, *14*, 1800612.

[26] a) S. Y. Lu, G. J. Xiao, L. Z. Sui, T. L. Feng, X. Yong, S. J. Zhu, B. J. Li, Z. Y. Liu, B. Zou, M. X. Jin, J. S. Tse, H. Yan, B. Yang, *Angew. Chem., Int. Ed.* **2017**, *56*, 6187; b) C. Liu, G. J. Xiao, M. L. Yang, B. Zou, Z. L. Zhang, D. W. Pang, *Angew. Chem., Int. Ed.* **2018**, *57*, 1893.

[27] P. T. Jing, D. Han, D. Li, D. Zhou, D. Z. Shen, G. J. Xiao, B. Zou, S. N. Qu, *Nanoscale Horiz.* **2019**, *4*, 175.

[28] a) D. Zhou, Y. C. Zhai, S. N. Qu, D. Li, P. T. Jing, W. Y. Ji, D. Z. Shen, A. L. Rogach, *Small* **2017**, *13*, 1602055; b) D. Li, C. Liang, E. V. Ushakova, M. H. Sun, X. D. Huang, X. Y. Zhang, P. T. Jing, S. J. Yoo, J. G. Kim, E. S. Liu, W. Zhang, L. H. Jing, G. C. Xing, W. T. Zheng, Z. K. Tang, S. N. Qu, A. L. Rogach, *Small* **2019**, *15*, 1905050.

[29] S. Y. Ma, L. Jin, X. Huang, C. Riziotis, R. Huang, C. L. Zhang, J. Lu, W. Q. Yang, *Adv. Mater. Interfaces* **2018**, *5*, 1800587.

[30] Y. L. Xu, L. Jin, X. B. He, X. Huang, M. L. Xie, C. F. Wang, C. L. Zhang, W. Q. Yang, F. B. Meng, J. Lu, *J. Mater. Chem. A* **2019**, *7*, 1810.

[31] H. J. Kim, J. H. Kim, K. W. Jun, J. H. Kim, W. C. Seung, O. H. Kwon, J. Y. Park, S. W. Kim, I. K. Oh, *Adv. Energy Mater.* **2016**, *6*, 1502329.

[32] S. W. Cui, Y. B. Zheng, J. Liang, D. A. Wang, *Chem. Sci.* **2016**, *7*, 6477.

[33] a) W. Z. Wu, Z. L. Wang, *Nat. Rev. Mater.* **2016**, *1*, 16031; b) W. Z. Wu, *Nanotechnology* **2016**, *27*, 112503; c) M. Wu, Y. X. Wang, S. J. Gao, R. X. Wang, C. X. Ma, Z. Y. Tang, N. Bao, W. X. Wu, F. R. Fan, W. Z. Wu, *Nano Energy* **2019**, *56*, 693.

[34] L. Jin, S. Y. Ma, W. L. Deng, C. Yan, T. Yang, X. Chu, G. Tian, D. Xiong, J. Lu, W. Q. Yang, *Nano Energy* **2018**, *50*, 632.

[35] M. Kundu, C. M. Costa, J. Dias, A. Maceiras, J. L. Vilas, S. Lanceros-Méndez, *J. Phys. Chem. C* **2017**, *121*, 26216.

[36] C. W. Xu, L. Zhang, Y. L. Xu, Z. Z. Yin, Q. Chen, S. Y. Ma, H. H. Zhang, R. Huang, C. L. Zhang, L. Jin, W. Q. Yang, J. Lu, *J. Mater. Chem. A* **2017**, *5*, 189.

[37] C. W. Xu, L. Jin, L. Zhang, C. F. Wang, X. Huang, X. B. He, Y. L. Xu, R. Huang, C. L. Zhang, W. Q. Yang, J. Lu, *Compos. Sci. Technol.* **2018**, *164*, 282.

[38] D. P. Zhang, P. F. Tian, X. Chen, J. Lu, Z. W. Zhou, X. M. Fan, R. Huang, *Compos. Sci. Technol.* **2013**, *77*, 29.

[39] C. Lu, L. Zhang, C. W. Xu, Z. Z. Yin, S. B. Zhou, J. X. Wang, R. Huang, X. Q. Zhou, C. L. Zhang, W. Q. Yang, J. Lu, *RSC Adv.* **2016**, *6*, 67400.

[40] P. Tian, C. Xu, H. Huang, X. Chen, L. Zhao, J. Lyu, *Gut* **2016**, *65*, 1260.

[41] A. Houachtia, P. Alcouffe, G. Boiteux, G. Seytre, J. F. Gérard, A. Serghei, *Nano Lett.* **2015**, *15*, 4311.

[42] Y. Lee, K. L. Kim, H. S. Kang, B. Jeong, C. Park, I. Bae, S. J. Kang, Y. J. Park, C. Park, *Small* **2018**, *14*, 1704024.

[43] Z. Y. Pi, J. W. Zhang, C. Y. Wen, Z. B. Zhang, D. P. Wu, *Nano Energy* **2014**, *7*, 33.

[44] V. Bhavanasi, D. Y. Kusuma, P. S. Lee, *Adv. Energy Mater.* **2014**, *4*, 1400723.

[45] M. Baniasadi, Z. Xu, S. Hong, M. Naraghi, M. Minary-Jolandan, *ACS Appl. Mater. Interfaces* **2016**, *8*, 2540.

[46] N. Meng, X. J. Zhu, R. Mao, M. J. Reece, E. Bilotti, *J. Mater. Chem. C* **2017**, *5*, 3296.

[47] S. Chen, X. M. Tao, W. Zeng, B. Yang, S. M. Shang, *Adv. Energy Mater.* **2017**, *7*, 1601569.

[48] A. C. Wang, Z. Liu, M. Hu, C. C. Wang, X. D. Zhang, B. J. Shi, Y. B. Fan, Y. G. Cui, Z. Li, K. L. Ren, *Nano Energy* **2018**, *43*, 63.

[49] B. Wunderlich, *Macromolecular Physics, Vol. 1, Crystal Structure, Morphology, Defects*, Academic Press, New York **1973**.

[50] Z. W. Pan, Z. R. Dai, C. Ma, Z. L. Wang, *J. Am. Chem. Soc.* **2002**, *124*, 1817.

[51] R. S. Yang, Z. L. Wang, *Philos. Mag.* **2007**, *87*, 2097.

[52] a) Z. L. Wang, J. Song, *Science* **2006**, *312*, 242; b) Y. Qin, X. Wang, Z. L. Wang, *Nature* **2008**, *451*, 809.

[53] S. Y. Xu, Y. W. Yeh, G. Poirier, M. C. McAlpine, R. A. Register, N. Yao, *Nano Lett.* **2013**, *13*, 2393.

[54] a) X. Yao, Y. L. Song, L. Jiang, *Adv. Mater.* **2011**, *23*, 719; b) M. J. Liu, S. T. Wang, L. Jiang, *Nat. Rev. Mater.* **2017**, *2*, 17036.

[55] A. S. Vaughan, *J. Mater. Sci.* **1993**, *28*, 1805.